Experimental Neurology 233 (2012) 523–533

Contents lists available at SciVerse ScienceDirect

Experimental Neurology

journal homepage: www.elsevier.com/locate/yexnr

Cilostazol, a phosphodiesterase inhibitor, prevents no-reflow and hemorrhage in mice with focal cerebral ischemia

Yoshiki Hase, Yoko Okamoto, Youshi Fujita, Akihiro Kitamura, Hitomi Nakabayashi, Hidefumi Ito, Takakuni Maki, Kazuo Washida, Ryosuke Takahashi, Masafumi Ihara *

Department of Neurology, Kyoto University Graduate School of Medicine, Kyoto, Japan

ARTICLE INFO

Article history:
Received 16 August 2011
Revised 5 November 2011
Accepted 25 November 2011
Available online 8 December 2011

Keywords:
Cilostazol
Focal cerebral ischemia
Matrix metalloproteinase
Virchow's triad
Tissue plasminogen activator

ABSTRACT

Background and Purpose: The Cilostazol Stroke Prevention Study II has shown a similar efficacy in stroke prevention but markedly fewer hemorrhagic events with the phosphodiesterase inhibitor cilostazol versus aspirin. The purpose of this study is therefore to investigate how cilostazol affects cerebral hemodynamics and whether it prevents hemorrhagic transformation induced by recombinant tissue plasminogen activator (rtPA) in a mouse model of focal ischemia/reperfusion. Particular emphasis will be placed on the plasma-microvessel interface.

Methods: After receiving food containing 0.3% cilostazol or standard food for 7 days, adult C57BL/6 J mice were subjected to middle cerebral artery occlusion/reperfusion with or without rtPA (10 mg/kg) intravenously administered prior to reperfusion. Cerebral blood flow was monitored at several time points by laser speckle imaging in the 24 hour period post reperfusion, before neurobehavioral and histological assessment. The long-term effect of cilostazol on cerebral ischemia was analyzed in the non-rtPA cohort.

Results: In the non-rtPA cohort, pretreatment by cilostazol significantly decreased the endothelial expression of adhesion molecules (P-selectin and intercellular adhesion molecule-1) and prevented platelet aggregation and leukocyte plugging in the microvessels after cerebral ischemia/reperfusion in the acute phase. Cilostazol significantly reduced mortality rate and improved motor function at 7 days post-ischemia/reperfusion. In the rtPA cohort, cilostazol significantly suppressed edema formation and hemorrhagic transformation with reduced density of microglial cells positive for matrix metalloproteinase-9 in the cerebral cortex and the striatum. In both cohorts, cilostazol significantly suppressed focal no-reflow, mitigated cerebral infarct, and improved neurological outcome.

Conclusions: Cilostazol may possess protective properties against cerebral ischemic injury by preventing no-reflow and hemorrhagic transformation, via maintenance of microvascular integrity.

Virchow's triad has been proposed to describe the vascular basis of ischemic injury in the central nervous system (del Zoppo, 2008). The triad elements consist of injury to vascular endothelium, abnormalities of hemorrheology, and reduction of flow within vascular bed. Their targets are blood vessels, blood elements (i.e., leukocytes, platelets, and coagulation/fibrinolysis system), and blood flow, respectively.

ts that agents that iad could be beneficial in reducing the consequences of ischemic injury instead of targeting just one element of the triad. In support of this hypothesis, targeting just one element–inhibition of platelet activation using an αIIbβ3 inhibitor resulted in symptomatic hemorrhage in rodent or nonhuman primate focal ischemia models (Abumiya et al., 2000). Thus, compounds that not only affect platelet function directly, but also indirectly, via action at the vascular wall, may prove useful. For instance, dipyridamole can inhibit platelet aggregation by direct action through a mechanism involving phosphodiesterase-5 but also indirectly by increasing endothelial cell-dependent adenosine concentrations (FitzGerald, 1987). Accordingly, the ESPRIT study indicated that the combination regimen of aspirin plus dipyridamole was superior to aspirin alone as antithrombotic therapy after cerebral ischemia of arterial origin (Halkes et al., 2006).

Another phosphodiesterase inhibitor, cilostazol, acts as an antiplatelet agent and has other pleiotropic effects based on phosphodiesterase-3-dependent mechanisms (Liu et al., 2001). Increasing evidence suggests that cilostazol offers endothelial protection, via an inhibition of

* Corresponding author at: Department of Neurology, Kyoto University Graduate School of Medicine, 54 Kawahara-cho, Shogoin, Sakyo, Kyoto 606–8507 Japan. Fax: +81 75 7514257.

E-mail addresses: hasecchi@kuhp.kyoto-u.ac.jp (Y. Hase), yoko416@kuhp.kyoto-u.ac.jp (Y. Okamoto), fujitauc@kuhp.kyoto-u.ac.jp (Y. Fujita), manto@kuhp.kyoto-u.ac.jp (A. Kitamura), baku@kuhp.kyoto-u.ac.jp (H. Nakabayashi), itohid@kuhp.kyoto-u.ac.jp (H. Ito), harutoma@kuhp.kyoto-u.ac.jp (T. Maki), kazw7@kuhp.kyoto-u.ac.jp (K. Washida), ryosuket@kuhp.kyoto-u.ac.jp (R. Takahashi), ihara@kuhp.kyoto-u.ac.jp (M. Ihara).

0014-4886
doi:10.1016/j.expneurol.2011.11.038

apoptosis in endothelial cells (Kim et al., 2002), attenuates the phenotypic modulation of vascular smooth muscle cells (Fujita et al., 2008), and sustains blood flow by endothelium-independent vasodilation (Tanaka et al., 1989). This suggests that cilostazol can affect not only blood elements, such as platelets, but also blood flow and blood vessel integrity, namely all the three elements of Virchow's triad. The recently published Cilostazol Stroke Prevention Study (CSPS)-II showed that cilostazol was, at least, noninferior to aspirin in the prevention of recurrent stroke in patients who had noncardioembolic stroke, and was safer than aspirin; however, cilostazol showed significantly increased side effects, i.e. diarrhea, headache, dizziness, palpitations, as compared to aspirin when used in secondary stroke prevention (Shinohara et al., 2010). Notably, patients taking cilostazol were significantly (54%) less likely to suffer a bleeding event, strengthening the notion that the drug not only has antiplatelet effects but also multifunctional roles that affect more than one target of Virchow's triad with respect to cerebral ischemia.

This study was therefore sought to address the mechanisms behind cilostazol's effect on Virchow's triad and any resultant neurovascular dysfunction after focal ischemia. We therefore assessed whether and, if so, how cilostazol improves the no-reflow phenomenon and how cilostazol prevents recombinant tissue plasminogen activator (rtPA)-induced hemorrhagic transformation in a mouse model of focal ischemia. Particular emphasis was given to the elements of the triad and the plasma-microvessel interface.

Materials and methods

Animals, treatments, and surgical procedures

The experimental protocol is described in Fig. 1. A total of 79 male C57BL/6 J mice (10–12 weeks old, weighing 24–29 g; CLEA Japan, Inc., Tokyo, Japan) were fed with the pelleted food containing 0.3% cilostazol (cilostazol-treated mice, n = 39) or pelleted food only (vehicle-treated mice, n = 40) for 7 days before the operation. All procedures were performed in accordance with the guidelines for animal experimentation from the ethical committee of Kyoto University. The mice were given access to food and water *ad libitum*. We performed middle cerebral artery occlusion/reperfusion (MCAO/R) without blockade of either common carotid artery or pterygopalatine artery blood flow. Detailed surgical procedures of MCAO/R are as follows: Mice were subjected to middle cerebral artery occlusion/reperfusion (MCAO/R) surgery after being anesthetized with 1.5% isoflurane in air. Body temperature was maintained at 37.0 ± 0.5 °C with the aid of feedback warming pad during operation. A midline incision was made in the neck, and the right common carotid artery (CCA), external carotid artery and internal carotid artery were isolated from the vagus nerve. Occipital, superior thyroid, lingual, maxillary arteries, and the external carotid artery were cauterized and cut so that the internal carotid artery and pterygopalatine artery (PPA) were visualized. The stump of the external carotid artery was cut and a filament made of 15 mm of 8–0 nylon string coated with silicon (180–200 μm diameter) was carefully advanced to 11 mm from the carotid artery bifurcation, or until resistance was encountered. We performed MCAO without blockade of either CCA or PPA blood flow (Chen et al., 2008). Approximately 60% reduction of CBF was achieved, as shown previously (Chen et al., 2008). After 45 or 90 minutes of MCAO, the filament was carefully withdrawn to induce vascular re-canalization/reperfusion.

Recombinant tissue plasminogen activator administration

rtPA (10 mg/kg alteplase dissolved with 150 μl of normal saline; Mitsubishi Tanabe Pharma Corporation, Osaka, Japan) was administered through tail vein immediately before reperfusion (45-minute MCAO/R plus rtPA, total n = 12 (cilostazol, n = 6; vehicle, n = 6), 90-minute MCAO/R plus rtPA, total n = 12 (cilostazol, n = 6; vehicle, n = 6)). The dose was in accordance with previous studies (Kollmar et al., 2004).

Measurement of cerebral blood flow

Relative CBF was determined by laser speckle perfusion imaging (Omegazone, Omegawave, Inc., Tokyo, Japan), which obtains high-

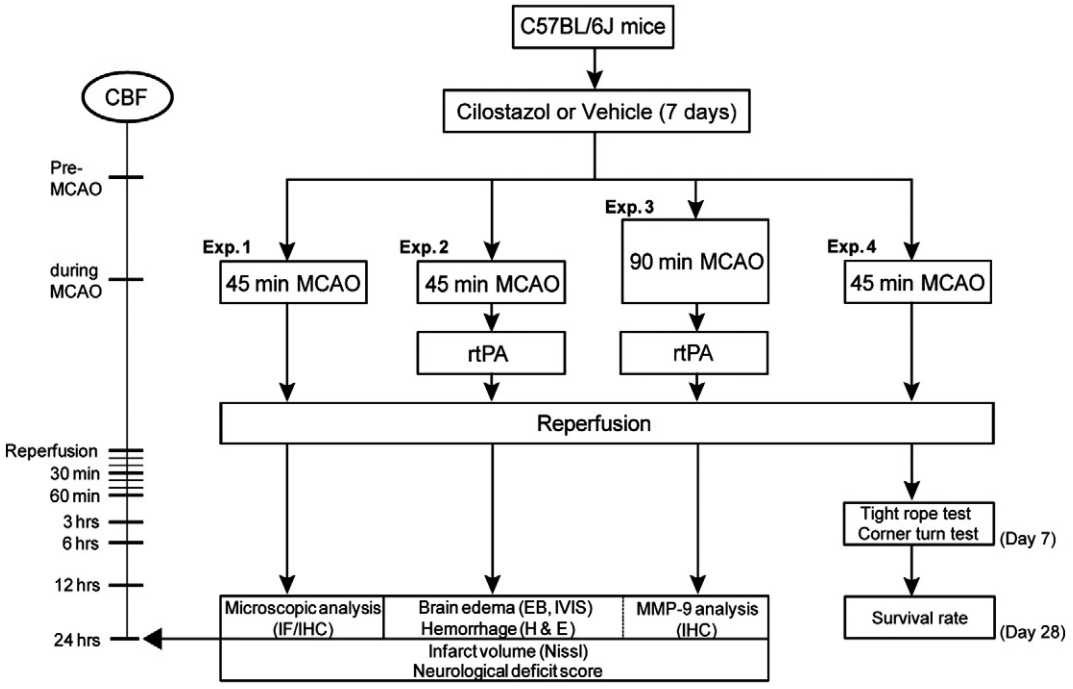

Fig. 1. Experimental protocol. MCAO, middle cerebral artery occlusion; CBF, cerebral blood flow; rtPA, recombinant tissue plasminogen activator; IF, immunofluorescence; IHC, immunohistochemistry; EB, Evans blue; MMP-9, matrix metalloproteinase-9. Exp. 1: total n = 20 (cilostazol, n = 10; vehicle, n = 10). Exp. 2: total n = 12 (cilostazol, n = 6; vehicle, n = 6). Exp. 3: total n = 12 (cilostazol, n = 6; vehicle, n = 6). Exp. 4: total n = 25 (cilostazol, n = 12; vehicle, n = 13).

resolution, two-dimensional imaging and has a linear relationship with absolute CBF values (Fujita et al., 2010). Recordings were performed through the skull under 1.5% isoflurane anesthesia. The periosteum, which adheres to the skull, was widely removed with fine-tip forceps. For each recording, the skull surface was wiped with saline-soaked gauze and then covered with a thin layer of gel (Aquasonic, Parker Laboratories, Inc., Fairfield, NJ) to prevent drying. Calibration was carried out with a calibration reference device (Calibrator S/N 080715-5, Omegawave, Inc., Tokyo, Japan) before each test. The mean CBF was measured in identically sized regions of interest (900 pixels) located 3 mm posterior and 2.5 mm lateral from the bregma. Five recordings of CBF were averaged and CBF values were expressed as a percentage of the preoperative value.

Motor function assessment

Twenty four hours after the surgery, mice (45-minute MCAO/R, total n = 20 (cilostazol, n = 10; vehicle, n = 10), 45-minute MCAO/R plus rtPA, total n = 12 (cilostazol, n = 6; vehicle, n = 6), 90-minute MCAO/R plus rtPA, total n = 10 (cilostazol, n = 5; vehicle, n = 5)) were examined for neurological deficits using a 5-point scale (Chan, 1994). Normal motor function was scored as 0, flexion of the contralateral torso and forelimb on lifting the animal by the tail as 1, circling to the contralateral side but normal posture at rest as 2, leaning to the contralateral side at rest as 3, and no spontaneous motor activity as 4. Scoring was performed by observers blinded to the procedure conducted on the animals. Data were analyzed by analysis of variance, followed by Mann–Whitney U analysis.

Latex perfusion method to assess arterial trunk patency

Mice (45-minute MCAO/R, total n = 10 (cilostazol, n = 5; vehicle, n = 5)) were deeply anesthetized with sodium pentobarbital (50 mg/Kg body weight) and a flexible catheter was inserted from the cardiac apex to the aorta. A mixture of 1 ml carbon black (Bokusai, Osaka, Japan), 10 ml LATEX (Chicago Latex, Crystal Lake, IL), and 10 ml normal saline was prepared and 4 ml infused through a flexible catheter at a constant pressure of 80 mmHg for 60 minutes after the surgery.

FITC-dextran injection to assess microvascular patency

To examine the patency of the cerebral microvessels, mice (45-minute MCAO/R, total n = 10 (cilostazol, n = 5; vehicle, n = 5)) were deeply anesthetized with sodium pentobarbital (50 mg/Kg body weight) and transcardially perfused with 0.1 g of FITC-dextran (2 x 10^6 molecular weight, Sigma, St. Louis, MO) diluted in 7.5 ml of normal saline at the pressure of 120 mmHg. The brains were then removed and fixed in 4% paraformaldehyde (PFA) in 0.1 mol/L PB (pH 7.4). Twenty μm-thick frozen coronal brain sections were made and examined under the fluorescence microscopy (BZ 9000; Keyence, Osaka, Japan).

Evaluation of brain edema and intracerebral hemorrhage

At 24 hours after MCAO/R with rtPA administration, mice (45-minute MCAO/R plus rtPA, total n = 10 (cilostazol, n = 5; vehicle, n = 5), 90-minute MCAO/R plus rtPA, total n = 10 (cilostazol, n = 5; vehicle, n = 5)) were injected with 2% Evans blue dye (Nacalai Tesque, Inc., Kyoto, Japan; diluted in 500 μl of normal saline) intraperitoneally. Two hours later, mice were deeply anesthetized with sodium pentobarbital (50 mg/Kg body weight) and perfused transcardially with normal saline until colorless perfusion fluid was obtained from the right atrium. The brains were then removed and fixed in 4% PFA in 0.1 mol/L PB (pH 7.4). Both the whole brain and 1.0 mm-thick coronally-cut brain sections were analyzed using IVIS® imaging system (Xenogen Caliper Life Sciences, Hopkinton, MA) (605 nm excitation and 680 nm emission) for quantitative analysis of Evans blue extravasation as an estimate of brain edema.

Using the same sections, the volume of intracerebral hemorrhage in every coronal section was calculated by the ABC/2 method (Kothari et al., 1996), as follows (mm^3): the major axis of the hemorrhage (mm) x minor axis of the hemorrhage (mm) x 1 mm (thickness) x 1/2. The volume in each section was then summed to calculate volume of intracerebral hemorrhage in each brain.

The evaluation was performed by an experimenter blind to the animal's group assignment.

Histopathology and immunohistochemistry

Animals were deeply anesthetized with sodium pentobarbital (50 mg/Kg body weight) and purfused transcardially at 20 ml/min with 0.01 mol/L PBS followed by 4% PFA. The brains were dissected out, and the coronally-cut brains were postfixed for 24 hours in 4% PFA in 0.1 mol/L PBS (pH 7.4). Fixed brains were dehydrated and embedded in paraffin. Six μm-thick brain sections were made, and antigen retrieval was performed by the following protocol: 15 minutes boiling in citrate buffer, pH 6.0 for intercellular adhesion molecule-1 (ICAM-1) and P-selectin, or autoclave at 121 °C for 30 minutes in citrate buffer, pH 6.0 for matrix metalloproteinase-9 (MMP-9), or autoclave at 121 °C for 10 minutes in citrate buffer, pH 6.0 for ionized calcium binding adapter molecule-1 (Iba-1). The sections were treated with primary antibodies against ICAM-1 (1:100, R&D systems, Minneapolis, MN), P-selectin (1:50, Santa Cruz Biotechnology, Santa Cruz, CA), MMP-9 (1:50, Santa Cruz) and Iba-1 (1:200, Wako, Osaka, Japan) overnight, followed by incubation with an appropriate secondary antibody (biotinylated anti-IgG; 1:100, Vector Laboratories, Burlingame, CA) for 1 hour and visualization with ABC Kit (Vector Laboratories).

Densitometric analysis for intercellular adhesion molecule-1 (ICAM-1) and P-selectin was carried out after immunohistochemistry (cilostazol, n = 6; vehicle, n = 6). Three different ROIs (0.4 mm^2) were drawn in the penumbral cortex and caudoputamen in close proximity to the lateral ventricle. After images of ICAM-1- and P-selectin-stained sections were captured, ICAM-1- and P-seleectin-positive capillaries were counted in each ROI and averaged.

The numerical density of the Iba-1-positive microglial cells and MMP-9-positive glial cells were counted in the whole cerebral cortex and the striatum of the brain section coronally cut at the bregma. The Iba-1-positive microglial cells with the minimal diameter of their cell bodies exceeding 7 or 10 μm were counted to assess the degree of activation of the microglial cells. The MMP-9-positive glial cells were also counted. After images of MMP-9- and Iba-1-stained sections were captured, areas (mm^2) of the cerebral cortex or striatum were measured by a computerized image system (ImageJ). The density of MMP-9- and Iba-1-positive cells was then calculated per area of the cerebral cortex or the striatum (/mm^2) (90-minute MCAO/R plus rtPA, total n = 12 (cilostazol, n = 6; vehicle, n = 6)).

Immunofluorescent staining

The brains that were fixed in 4% PFA in 0.1 mol/L PB and stored in 20% sucrose in 0.1 mol/L PBS (pH 7.4) after FITC-dextran injection were snap-frozen and 20 μm-thick brain sections were made. The sections were treated with antibodies against ICAM-1 (1:100), P-selectin (1:50), CD45 (1:50, BD Biosciences, San Jose, CA), and CD41 (1:50, BD Biosciences) overnight followed by incubation with rhodamine-conjugated rabbit polyclonal antibody to goat IgG H&L (1:50, Abcam, Cambridge, UK) for CD45 and CD41 or DyLight TM 405-conjugated rabbit polyclonal anti-rat IgG H&L (1:50, ROCKLAND, Gilbertsville, PA) for ICAM-1 and P-selectin. By using paraffin embedded brains, 6 μm-thick coronal brain sections were made, and antigen retrieval

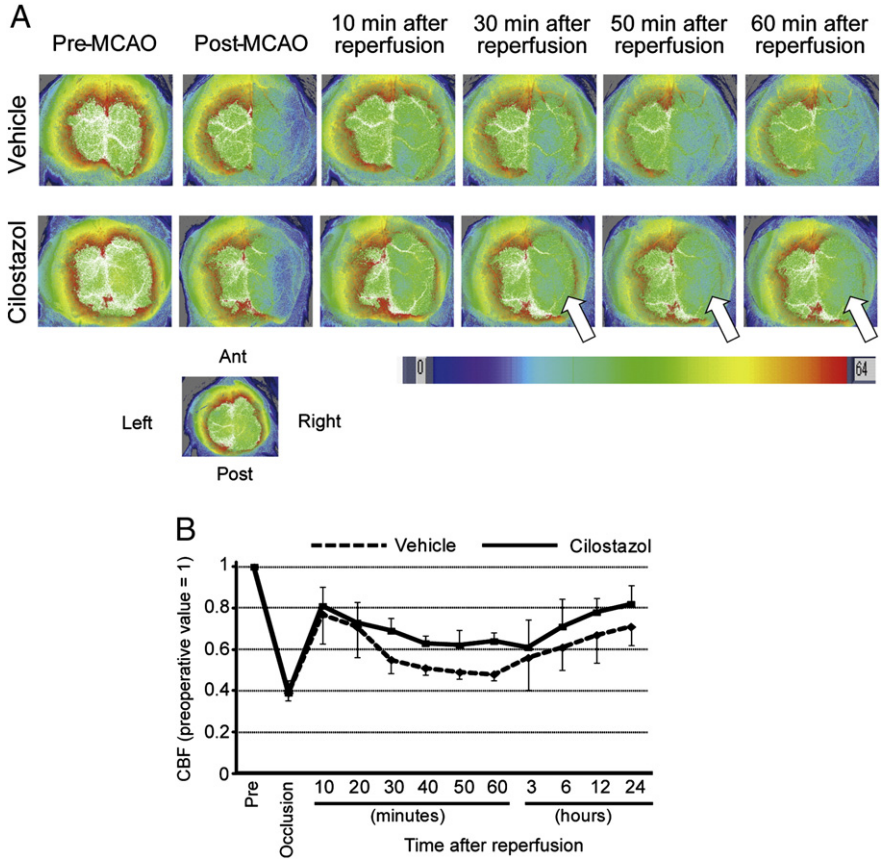

Fig. 2. Cilostazol suppressed no-reflow phenomenon. A, Representative images of cerebral blood flow (CBF) at the indicated time points pre- and post-MCAO/R in vehicle- and cilostazol-treated mice. Arrows indicate suppression of no-reflow phenomenon with cilostazol. B, Temporal profile of CBF of vehicle- and cilostazol-treated mice after 45-minute MCAO/R. CBF was expressed as a ratio to the baseline level (n = 5 each, $P<0.05$).

was performed by autoclave at 121 °C for 30 minutes in citrate buffer, pH 6.0 for MMP-9 and Iba-1. Double immunofluorescent staining was performed using primary antibodies against MMP-9 (1:50, Santa Cruz) and Iba-1 (1:200, Wako) with appropriate fluorescence-labeled secondary antibodies: Alexa Fluor 647 donkey polyclonal anti-goat IgG H&L (1:500, Invitrogen, Carlsbad, CA) for MMP-9 and DyLight TM 488-conjugated donkey polyclonal anti-rabbit IgG H&L (1:400, Jackson Immunoresearch, West Grove, PA) for Iba-1.

Densitometric analysis for microthrombi (CD41) and leukocytes (CD45) in the microvessels was carried out using immunofluorescent staining (cilostazol, n = 6; vehicle, n = 6). Three different ROIs (0.4 mm^2) were drawn in the penumbral cortex and caudoputamen in close proximity to the lateral ventricle. After images of CD41- and CD45-stained sections were captured, the density of CD41-positive microthrombi was measured by a computerized image system (ImageJ) and CD45-positive leukocytes inside the capillaries were counted in each ROI and averaged.

The co-localization ratio of MMP-9 (red) with Iba-1-positive microglia (green) was calculated in the cerebral cortex and caudoputamen at 24 hours after 90-minute MCAO/R plus rtPA (cilostazol, n = 6; vehicle, n = 6). Three different ROIs were drawn in the cerebral cortex and caudoputamen, where MMP-9 was well expressed. Thus, the ratio of MMP-9 positivity among the Iba-1-positive microglia was measured in each ROI and averaged.

Nissl staining

Four serial 2-mm-thick coronal sections between bregma coordinates +2 and −4 were obtained in a cutting block. Each block was embedded in paraffin and 6 μm-thick sections were cut from the caudal side of the block before being subjected to Nissl staining. Images were captured and infarct area was measured (mm^2) in each slice by a computerized image system (ImageJ). The infarction area in each slice x distance between slices (2 mm) were summed to approximate volume of infarct in each brain (mm^3).

Assesment of long-term effect of cilostazol against cerebral ischemia

After 45-minute MCAO/R, mice (total n = 25 (cilostazol, n = 12; vehicle, n = 13)) were observed for 28 days to analyze survival rate. Seven days after the surgery, tight rope (Gerber et al., 2001) and corner turn (Zhang et al., 2002) tests were carried out to analyze any subtle differences in motor coordination (45-minute MCAO/R, total n = 12 (cilostazol, n = 8; vehicle, n = 4)).

Tight rope test: Mice were taken by the tail and placed with their front paws in the middle of a 60 cm-long tight rope about 60 cm above the floor. A box with a padded floor was placed beneath the rope to prevent falling mice being injured. Healthy mice placed on the rope attempted to reach one end of the rope, usually by using

Fig. 3. Cilostazol preserved microvascular patency by suppressing platelet aggregation and leukocyte plugging in microvessels. A and B, Representative fluorescent images of the coronal sections of the brain perfused with FITC-dextran (green) of vehicle- (A) and cilostazol-treated mice (B) after 45-minute MCAO/R. Note the limited perfusion of FITC-dextran in the cortex or the striatum of the vehicle-treated mice (A, arrows). C, Densitometric analysis of the brain perfused with FITC-dextran of vehicle- and cilostazol-treated mice after 45-minute MCAO/R (n = 5 each). D, E, G, and H, Representative images of immunofluorescent staining for CD41 (D and E, red), CD45 (G and H, red), P-selectin (D and E, blue), and ICAM-1 (G and H, blue) of vehicle- (D, G) and cilostazol-treated (E, H) mice. Capillary is visualized with FITC-dextran (D, E, G, and H, green). F and I, Histograms showing the densitometric quantification of the CD41-positive micro-thrombi (F) and CD45-positive leukocytes (I) in the cerebral cortex (Cx) and in the caudoputamen (CP) of the vehicle- and cilostazol-treated mice (n = 5 each). J and K, Densitometric analysis of vessels positive for P-selectin (J) and ICAM-1 (K) (n = 6 each). Scale bars, 1 mm in A and B, 30 μm in D, E, G, and H.

their hind paws and tail for climbing. A tight rope test performance score was given based on whether the animal reached the end of the rope and the time required. A mouse climbing the platform at the side of the rope within 6 s received a score of 0. For each additional 6 s necessary to reach the platform, mice received one additional point. Mice hanging for 60 s at the rope without reaching the platform received a score of 10. Mice that fell from the rope before 60 s received one additional point for each 6 s missing from 60 s (i.e., a mouse unable to stay at the rope received a score of 20); thus, a low score indicated good performance in the tight rope test. All

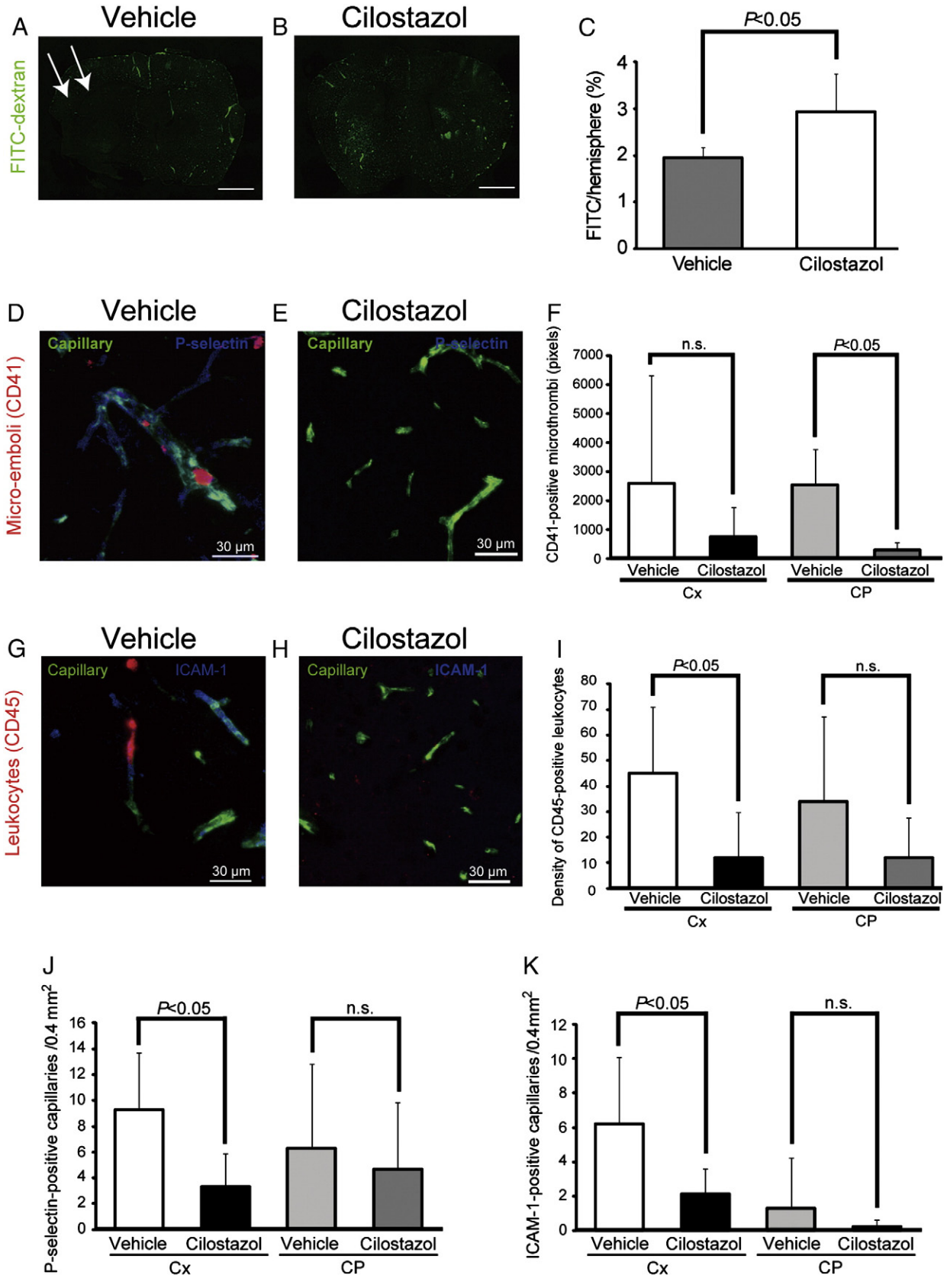

mice were tested twice per time point and their respective scores were used for statistical analysis.

Corner turn test: In the home cage, a mouse was placed between two boards each with dimension of 30 cm x 20 cm x 1 cm. The edges of the two boards were attached at a 30° angle with a small opening along the joint between the two boards to encourage entry into the corner. The mouse was placed between the two angled boards facing the corner and half way to the corner. When entering deep into the corner both sides of the vibrissae were stimulated together. The mouse then rears forward and upward, then turns back to face the open end. The model predicts that the non-ischemic mouse turn either left or right, but the ischemic mouse preferentially turns toward the non-impaired, ipsilateral (right) side. Turning movements that were not part of a rearing movement were not scored. The turns in one versus the other direction were recorded from ten trials for each test and the number of right turns was calculated.

Statistical analysis

All values are expressed as means ± SD in the text and figures. Unpaired *t*-test or one-way ANOVA was used to evaluate significant differences among groups, except where stated, followed by post-hoc Tukey's test or Tukey-Kramer's test. Temporal profiles of CBF were analyzed by two-way repeated measures ANOVA followed by a post-hoc Tukey's test. Differences with $P<0.05$ were considered statistically significant in all analyses.

Results

Mortality rate was less than 10% in the non-rtPA and the rtPA cohort at 24 hours after the surgery

In the non-rtPA cohort, the mortality rate was 9.1% (1 of 11) in vehicle-treated mice and 0% (0 of 10) in cilostazol-treated mice at 24 hours after the surgery. In the rtPA cohort, all of the 24 mice survived until 24 hours after the surgery.

Cilostazol suppressed no-reflow phenomenon in 45-minute MCAO/R

In both vehicle- and cilostazol-treated mice, CBF decreased to approximately 40% of its preoperative level during MCAO (Figs. 2A, B). Ten minutes after reperfusion, CBF recovered to around 80% of its preoperative level. However, beginning at 20 minutes after reperfusion, CBF gradually decreased despite vascular recanalization in vehicle-treated mice (n = 5), indicative of no-reflow phenomenon. In cilostazol-treated mice, the no-reflow phenomenon was significantly suppressed; the degree of CBF reduction was also less apparent during the 60 minute period after reperfusion. CBF began to recover at 3 hours after reperfusion and continued at least until 24 hours after reperfusion. The CBF recovery was significantly greater in the cilostazol-treated group ($P<0.05$). CBF recovered to approximately 80% of its preoperative level in the cilostazol-treated mice, but to 70% in vehicle-treated mice at 24 hours after reperfusion.

Cilostazol preserved microvascular blood flow in ischemic area by preventing microvascular obstruction by leukocytes and microthrombi in 45-minute MCAO/R

Latex perfusion analyses showed that the main MCA trunk was patent both in the vehicle- and cilostazol-treated mice, after MCAO/R. Therefore, the cilostazol-induced suppression of the no-reflow phenomenon is not considered to be linked to occlusion or stenosis of the main trunk of MCA; this therefore led us to focus on plasma-microvessel interface. In vehicle-treated mice, capillaries in ischemic regions were not sufficiently perfused with FITC-dextran with perfusion pressure reaching 120 mmHg. In cilostazol-treated mice, however, a greater number of capillaries were filled with FITC-dextran (Figs. 3A–C). Cilostazol-treated mice exhibited less capillary micro-thrombi formation in the striatum (Figs. 3D–F) and fewer lodged leukocytes in the capillaries of the cerebral cortex (Figs. 3G–I). Moreover, cilostazol-treated mice exhibited less expression of endothelial adhesion molecules, such as intercellular adhesion molecule-1 (ICAM-1) and P-selectin, in the ischemic cerebral cortex (Figs. 3J, K).

Cilostazol reduced infarct volume and improved motor function after 45-minute MCAO/R

Cilostazol-treated mice showed significantly less infarct volume (Figs. 4A–C) and better motor function (Fig. 4D).

Cilostazol promoted faster CBF recovery after 45-minute MCAO/R plus rtPA

After 45-minute MCAO/R plus rtPA, CBF decreased to approximately 40% of its preoperative level during MCAO in both vehicle and cilostazol-treated mice. At 10 minutes after reperfusion, CBF recovered to approximately 70% of its preoperative level in cilostazol-treated mice, but remained below 60% in vehicle-treated mice (Fig. 6A). Beginning at 20 minutes, CBF gradually decreased despite vascular recanalization at least until 1 hour after reperfusion. However, cilostazol-treated mice exhibited slightly increased CBF during this period. At 3 hours after reperfusion, the downward trend was reversed, with cilostazol-treated mice showing faster CBF recovery. Cilostazol-treated mice showed significantly better recovery of CBF ($P<0.05$).

Cilostazol ameliorated brain edema and hemorrhagic transformation after 45- or 90-minute MCAO/R plus rtPA

Using the IVIS® imaging system, whole brain analysis of extravasated Evans blue dye was conducted. Cilostazol-treated mice showed a nonsignificant trend toward less rtPA-induced brain

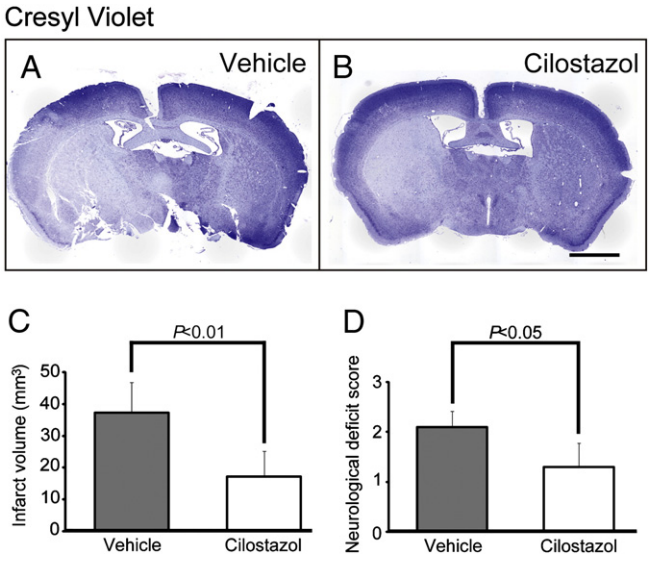

Fig. 4. Cilostazol reduced infarct volume and ameliorated neurological deficits. A and B, Representative images of Nissl staining of the brain of vehicle-treated (A) and cilostazol-treated (B) mice after 45-minute MCAO/R. C and D, Histograms showing the infarct volume (mm^3) (C) (cilostazol, n = 6; vehicle, n = 9) and the neurological deficit score (D) (n = 10 each) of the vehicle- or cilostazol-treated mice at 24 hours after 45-minute MCAO/R. Scale bars, 1 mm.

edema after 45-minute MCAO/R and significantly less brain edema after 90-minute MCAO/R (Figs. 5A–C). rtPA administration induced intracerebral hemorrhage in most of the vehicle-treated mice after 45-minute (in 4 out of 5 mice) and 90-minute (in all 5 mice) MCAO/R. Cilostazol almost completely prevented the hemorrhagic transformation and significantly reduced the volume of rtPA-induced hemorrhage in both cohorts (Figs. 5D–F).

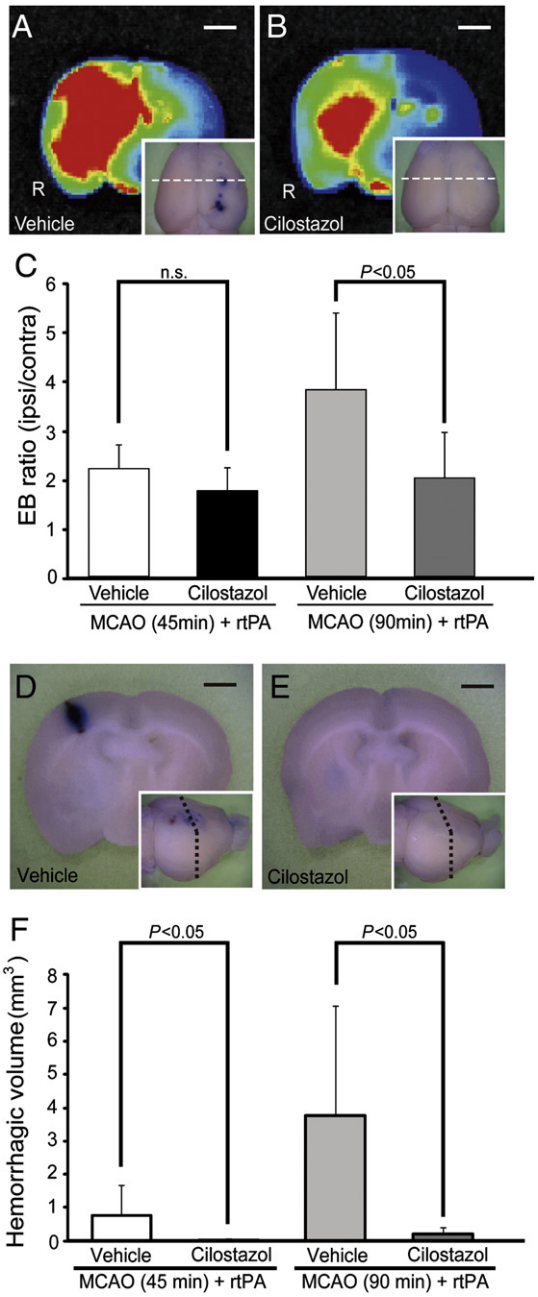

Fig. 5. Cilostazol reduced rtPA-induced brain edema and hemorrhagic transformation. A and B, Representative IVIS® images of coronal brain sections of vehicle-treated (A) and cilostazol-treated (B) mice injected with Evans blue at 24 hours after 90-minute MCAO/R plus rtPA. Insets show representative dorsal view of the brain. C, Histogram showing ipsilateral-to-contralateral ratio of Evans blue extravasation of vehicle-treated and cilostazol-treated mice at 24 hours after 45-minute (n = 5 each) or 90-minute (n = 5 each) MCAO/R plus rtPA. D and E, Representative images of coronal brain sections of vehicle-treated (D) and cilostazol-treated (E) mice at 24 hours after 90-minute MCAO/R plus rtPA. Insets show representative laterodorsal view of the brain. F, Histogram showing hemorrhagic volume of vehicle-treated and cilostazol-treated mice at 24 hours after 45-minute (n = 5 each) or 90-minute (n = 5 each) MCAO/R plus rtPA. Scale bars, 1 mm.

Cilostazol suppressed microglial activation and MMP-9 expression in the microglia

After 90-minute MCAO/R plus rtPA, activated microglial cells expressed matrix metalloproteinase-9 (MMP-9) in ischemic areas of both the cerebral cortex and caudoputamen in vehicle-treated mice (Figs. 6B, D). Cilostazol significantly attenuated such microglial activation (Figs. 6C, G, and H) and MMP-9 expression compared to vehicle-treated mice (Figs. 6E, F).

Cilostazol reduced infarct volume and improved motor function after 45- or 90-minute MCAO/R with rtPA administration

Cilostazol-treated mice showed significantly less infarct volume (Figs. 7A–E) and better motor function at 24 hours after 45- or 90-minute MCAO/R plus rtPA (Fig. 7F).

Cilostazol reduced a mortality rate during the 28-day period after 45-minute MCAO/R

In vehicle-treated mice, the mortality rate was 69% (9 of 13) at 7 days, and 85% (11 of 13) at 28 days after 45-minute MCAO/R. However, in cilostazol-treated mice, the mortality rate was 25% (3 of 12) at 7 days, and 33% (4 of 12) at 28 days after surgery. Cilostazol significantly reduced a mortality rate until 28 days after 45-minute MCAO/R (Kaplan-Meier survival analysis, log-rank $P<0.01$) (Fig. 8A).

Cilostazol improved motor function at 7 days after 45-minute MCAO/R

The performance in the tight rope test was significantly improved in cilostazol-treated mice compared to vehicle-treated mice at 7 days after 45-minute MCAO/R (Fig. 8B). In the corner turn test, cilostazol-treated mice showed a significant decrease in the right turns compared to vehicle-treated mice at 7 days after 45-minute MCAO/R (Fig. 8C).

Discussion

This study using a mouse model of focal cerebral ischemia showed that cilostazol: (1) preserved microvascular patency by decreasing the endothelial expression of P-selectin and ICAM-1 and therefore prevented platelet aggregation and leukocyte plugging in microvessels in the acute phase in the non-rtPA cohort, which subsequently lead to a reduced mortality rate and improved motor function in a later phase; (2) ameliorated rtPA-induced brain edema and hemorrhagic transformation at least partially due to suppression of microglial MMP-9 expression in the rtPA cohort; (3) suppressed focal no-reflow, mitigated cerebral infarct, and improved neurological outcome in both cohorts. Such pleiotropic effects of cilostazol, that are at least partially exerted by vascular protection, may explain the effectiveness of CSPS (Gotoh et al., 2000), CASISP (Huang et al., 2008), and CSPS-II (Shinohara et al., 2010).

Early restoration of antegrade flow is expected to enhance the functional recovery after stroke. However, recent studies have demonstrated that successful reopening of an occluded artery with rtPA does not necessarily lead to clinical improvement (Alexandrov et al., 2004); such phenomenon is explained by several potential mechanisms, including edema formation (von Kummer et al., 2001), hemorrhagic transformation (Alexandrov and Grotta, 2002), no-reflow phenomenon (del Zoppo and Hallenbeck, 2000), proximal reocclusion (Alexandrov and Grotta, 2002), and reperfusion injury (Uematsu et al., 1989). Such predisposing factors warrant treatment as delayed recovery of brain function may still occur in these patients with 'ischemic stunning of the brain' (Alexandrov et al., 2004). Such predisposing factors may be closely linked with the three elements of the Virchow's triad: 1) blood vessels are linked with edema/

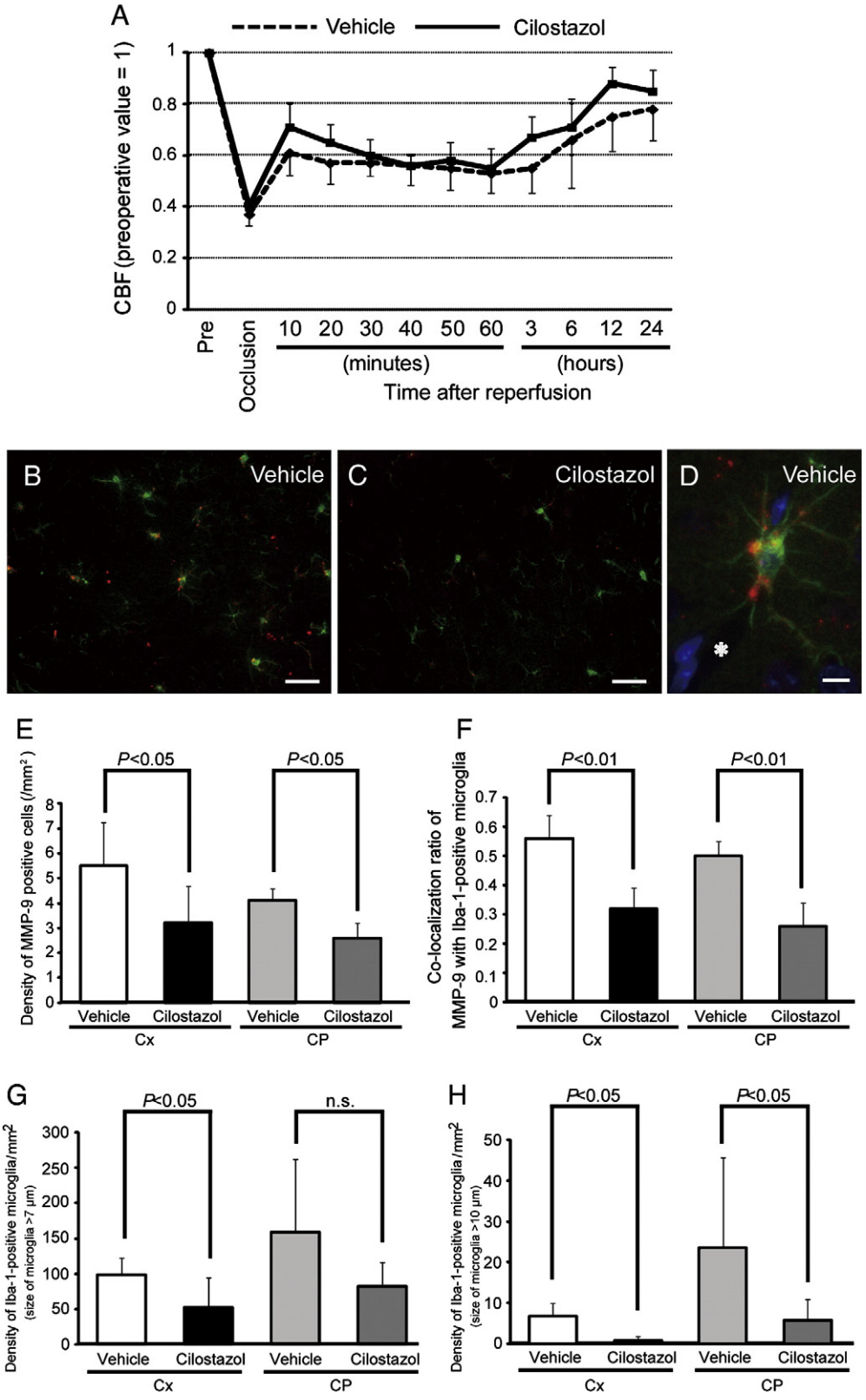

Fig. 6. Cilostazol promoted faster recovery of cerebral blood flow and reduced MMP-9 positive activated microglia after MCAO/R plus rtPA. A, Temporal profile of cerebral blood flow (CBF) of vehicle- and cilostazol-treated mice after 45-minute MCAO/R plus rtPA (n = 5 each, $P<0.05$). The preoperative CBF value was set as 1. B–D, Representative images of immunofluorescent staining for MMP-9 (red) and Iba-1-positive microglia (green) in ischemic cortical hemisphere of vehicle-treated (B, D) and cilostazol-treated (C) mice at 24 hours after 90-minute MCAO/R plus rtPA. An enlarged microglial cell with thickened processes secretes MMP-9 around a vessel (D, asterisk). Nuclei are stained with DAPI (D, blue). E and F, Histograms showing the density of MMP-9-positive cells per mm^2 (E) and co-localization ratio of MMP-9 with Iba-1-positive microglial cells (F) in the cerebral cortex (Cx) and the caudoputamen (CP) of the vehicle-treated and cilostazol-treated mice at 24 hours after 90-minute MCAO/R plus rtPA (n = 6 each). G and H, Histograms showing the density (/mm^2) of 'activated' microglia, with a cell body size exceeding 7 μm (G) and 'highly activated' microglia, with a cell body size exceeding 10 μm (H) in the ischemic cerebral cortex (Cx) and caudoputamen (CP) of the vehicle- or cilostazol-treated mice after 90-minute MCAO/R plus rtPA (n = 6 each). Scale bars, 40 μm (B, C), 10 μm (D).

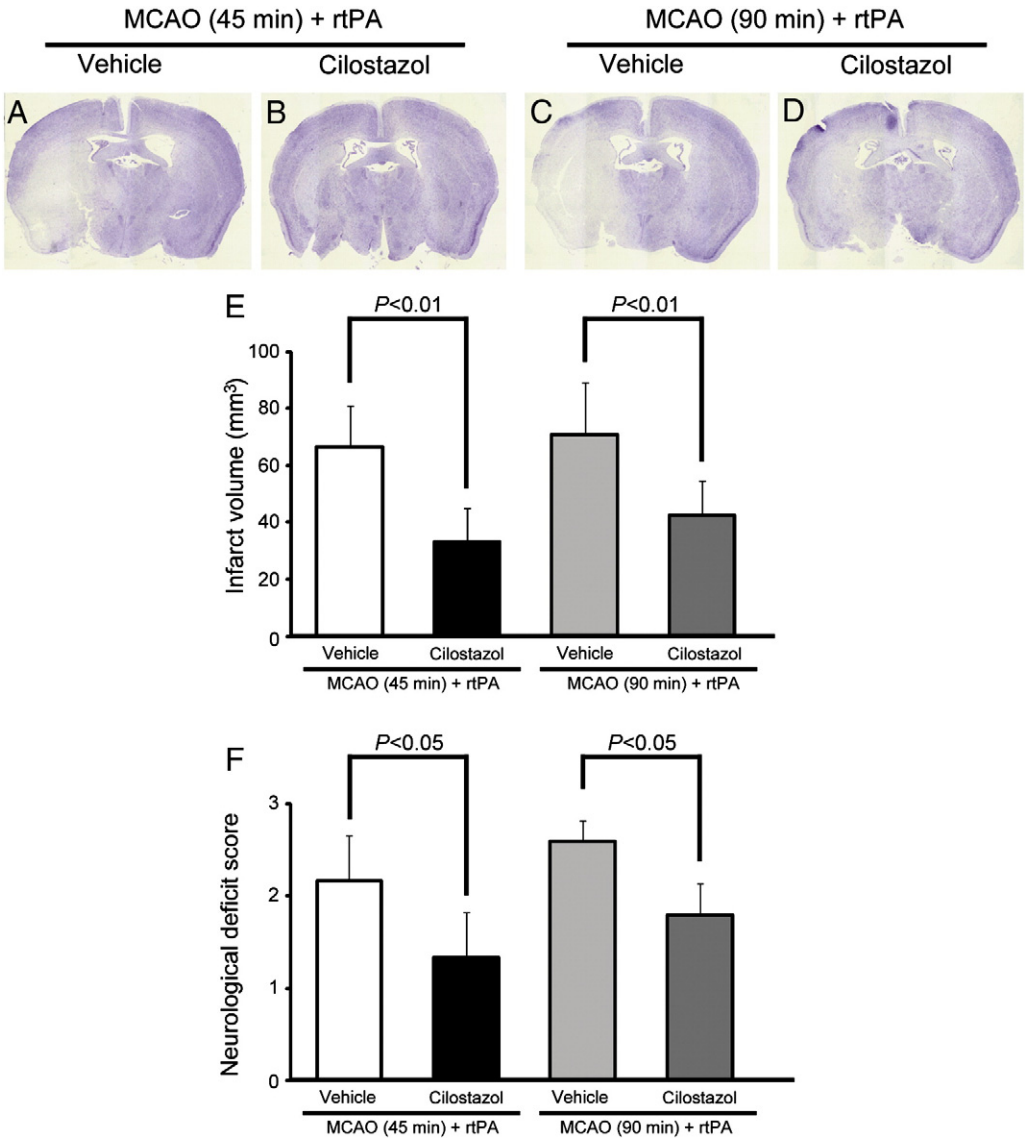

Fig. 7. Cilostazol reduced infarct volume and ameliorated neurological deficits after MCAO/R plus rtPA. A–D, Representative images of Nissl staining of the coronally-cut brain of the vehicle-treated (A, C) or cilostazol-treated (B, D) mice at 24 hours after 45-minute (A, B) or 90-minute (C, D) MCAO/R in combination with rtPA. E and F, Histograms showing the infarct volume (mm^3) (E) (45-minute MCAO/R plus rtPA, n = 5 each; 90-minute MCAO/R plus rtPA, n = 5 each) and the neurological deficit score (F) (45-minute MCAO/R plus rtPA, n = 6 each; 90-minute MCAO/R plus rtPA, n = 5 each) of the vehicle- or cilostazol-treated mice at 24 hours after 45-minute or 90-minute MCAO/R plus rtPA.

hemorrhage formation or reperfusion injury; 2) blood flow is associated with no-reflow phenomenon; and 3) blood elements are associated with proximal reocclusion. Therefore, these three elements would be a suitable starting point when considering a combination therapy with rtPA. In addition, platelet hyperaggregability may ensue after rtPA therapy (Ohlstein et al., 1987), providing a rationale of using antiplatelet drug such as cilostazol to salvage ischemic stunning of the brain after rtPA therapy.

Several studies have reported the neuroprotective roles of cilostazol in acute brain injury in experimental rodent models of MCAO/R. Following 2-hour MCAO/R in Sprague–Dawley rats, post-ischemic administration of cilostazol resulted in reduction of infarct volume with reduced apoptosis and upregulated bcl-2 (Choi et al., 2002; Lee et al., 2004). Another study showed cilostazol, given immediately after 45-min MCAO/R, mitigated infarction and enhanced neurogenesis in C57BL/6 mice (Tanaka et al., 2010). This protection was achieved by a cAMP response-element-binding protein-mediated signaling pathway, without CBF changes at 1, 3, and 7 days after reperfusion (Tanaka et al., 2010). Thus, cilostazol may protect against ischemic neuronal damage through its cAMP-elevating activity even without CBF changes. However, since the above studies did not evaluate CBF within 1 day after reperfusion, there is still a possibility that cilostazol exerted a neuroprotective role by restoring CBF in an earlier phase after reperfusion. By monitoring CBF in the 24 hours, our study showed that cilostazol suppressed the no-reflow phenomenon by restoring microvascular circulation at an earlier phase. In accordance with this result, in a different experimental paradigm using photothrombotic permanent MCAO in spontaneously hypertensive rats, cilostazol given 2 hours before or 30 min after MCAO significantly reduced infarct volume; this was accompanied by increased CBF at 1- and 2-hour post-MCAO (Ito et al., 2010).

A recent study has reported that cilostazol prevented rtPA-induced hemorrhagic transformation, brain edema, and endothelial injury at 18 hours after reperfusion in ddY mice with 6-hour MCAO/R (Ishiguro et al., 2010). Although CBF was not examined in the previous study, the notable effects of cilostazol were explained by reduced MMP-9 activity and restored claudin-5 expression. This is consistent with our results, which showed that cilostazol may protect the blood–brain barrier (BBB) by downregulating the microglial MMP-9

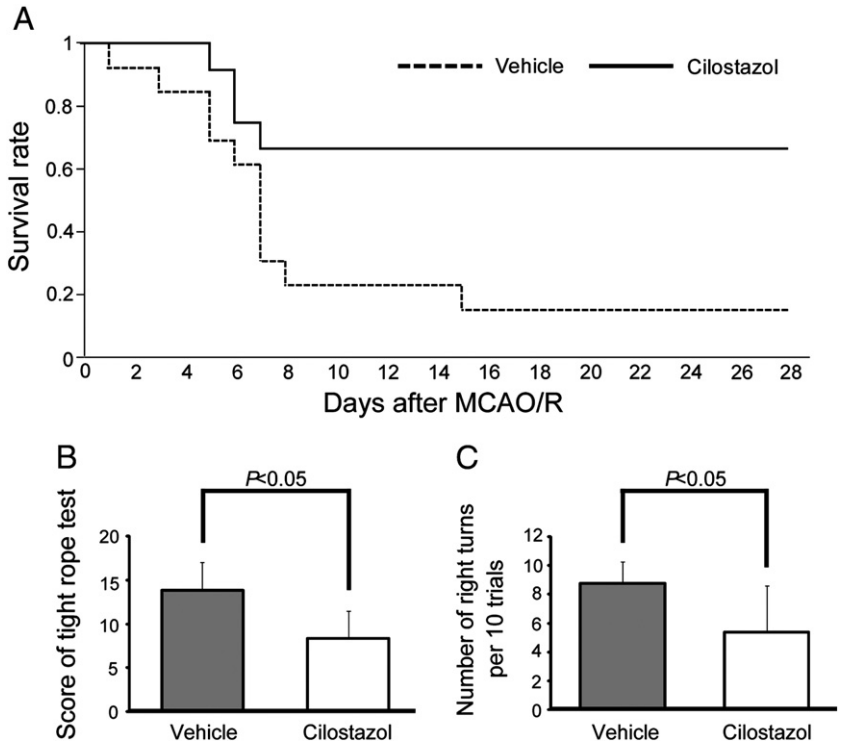

Fig. 8. Cilostazol reduced a mortality rate and improved motor function. A, Kaplan-Meier survival analysis after 45-minute MCAO/R, showing that cilostazol significantly reduced a mortality rate during the following 28 days (cilostazol, n = 12; vehicle, n = 13; log-rank $P<0.01$). B and C, Histograms showing the score of the tight rope test (B) and the number of right turns in the corner turn test (C) at 7 days after 45-minute MCAO/R (cilostazol, n = 8; vehicle, n = 4).

expression. Alternatively, cilostazol may have a direct protective effect on vasculature given the absence of any difference in brain edema but the presence of significant difference in hemorrhagic volume between vehicle- and cilostazol-treated groups after 45-minute MCAO/R plus rtPA.

Previous reports indicate that cerebral ischemia activates MCP-1 production via NF-κB signaling pathway (Liu et al., 2001) or activates mitogen-activated protein kinases (Maddahi et al., 2009), both leading to MMP-9 activation. rtPA is also known to increase MMP-9 through induction of low-density lipoprotein receptor-related protein (Wang et al., 2003). Given that cAMP suppresses NF-κB, MCP-1, and mitogen-activated protein kinases (Tsai et al., 2008), cilostazol may prevent BBB leakage via MMP-9 inhibition. Thus, besides its antiplatelet activity, cilostazol has a role in restoring CBF and protecting endothelial function, making it a candidate drug for a combination therapy with rtPA.

The long-term effects of cilostazol warrant further investigation using a focal ischemia model of 45-minute MCAO/R. Previous reports indicate that a mortality rate at 7 days is more than 50% after 60-minute MCAO/R (Komine-Kobayashi et al., 2004) and 100% after 6-hour MCAO/R (Ishiguro et al., 2010). As expected, in vehicle-treated mice, a mortality rate was high, measuring 69% at 7 days, and 85% at 28 days after 45-minute MCAO/R, in accordance with the previous report (Komine-Kobayashi et al., 2004). However, in cilostazol-treated mice, the mortality rate was 25% at 7 days, and 33% at 28 days after the surgery. Cilostazol significantly reduced the mortality rate during 28 days after 45-minute MCAO/R; this could thus be deduced as a neuroprotective effect of cilostazol. Because a high mortality rate was anticipated after 45-minute MCAO/R, neurobehavioral assessment was carried out at 7 days after the surgery. Cilostazol-treated mice showed significantly better performance in the tight rope test and the corner turn test although confounded by a survival bias. Thus, long-term effect of cilostazol against ischemic stroke was demonstrated.

A limitation of this study is that cilostazol was administered prior to induction of MCAO/R to obtain its stable blood concentration. However, cilostazol is known to show maximal plasma levels at 2 to 4 hours after oral administration in rats, and pre-ischemic and post-ischemic administration of cilostazol were almost equally effective to mitigate infarction in permanent MCAO model (Ito et al., 2010). Therefore, post-ischemic administration of cilostazol might be also effective against no-reflow phenomenon in transient focal ischemia. If extrapolated clinically, the current study suggests that cilostazol could be a promising drug for secondary prevention of stroke by minimizing focal brain ischemia and rtPA-induced BBB leakage in preparation for any subsequent stroke. In acute clinical settings, however, it remains to be elucidated whether post-ischemic administration of cilostazol, with or without concomitant rtPA, ameliorates the no-reflow phenomenon.

In conclusion, cilostazol can be considered a safe and beneficial vasculo- and neuroprotective agent that affects different components of the ischemic cascade and enhances the therapeutic effects of thrombolysis by restoring the integrity of the plasma-vessel interface.

Source of funding

This work was supported by a Grant-in-Aid for Exploratory Research from the Japanese Ministry of Education, Culture, Sports, Science and Technology (M.I., No. 22650073), and by the Research fund from the Otsuka Pharmaceutical Co. Ltd. (Tokyo, Japan).

Disclosures

The study is designed, conducted, analyzed, and reported independently of the funding agencies and pharmaceutical companies, although cilostazol was supplied by Otsuka Pharmaceutical Co. Ltd. and alteplase by Mitsubishi Tanabe Pharma Corporation (Osaka, Japan).

Acknowledgment

The authors are grateful to Dr. Ahmad Khundakar for his insightful comments. We also thank Ms. Takako Kawada for assistance in staining the tissue sections.

References

Abumiya, T., Fitridge, R., Mazur, C., Copeland, B.R., Koziol, J.A., Tschopp, J.F., Pierschbacher, M.D., del Zoppo, G.J., 2000. Integrin alpha(IIb)beta(3) inhibitor preserves microvascular patency in experimental acute focal cerebral ischemia. Stroke 31, 1402–1409 discussion 1409–1410.

Alexandrov, A.V., Grotta, J.C., 2002. Arterial reocclusion in stroke patients treated with intravenous tissue plasminogen activator. Neurology 59, 862–867.

Alexandrov, A.V., Hall, C.E., Labiche, L.A., Wojner, A.W., Grotta, J.C., 2004. Ischemic stunning of the brain: early recanalization without immediate clinical improvement in acute ischemic stroke. Stroke 35, 449–452.

Chan, P.H., 1994. Oxygen radicals in focal cerebral ischemia. Brain Pathol. 4, 59–65.

Chen, Y., Ito, A., Takai, K., Saito, N., 2008. Blocking pterygopalatine arterial blood flow decreases infarct volume variability in a mouse model of intraluminal suture middle cerebral artery occlusion. J. Neurosci. Methods 174, 18–24.

Choi, J.M., Shin, H.K., Kim, K.Y., Lee, J.H., Hong, K.W., 2002. Neuroprotective effect of cilostazol against focal cerebral ischemia via antiapoptotic action in rats. J. Pharmacol. Exp. Ther. 300, 787–793.

del Zoppo, G.J., 2008. Virchow's triad: the vascular basis of cerebral injury. Rev. Neurol. Dis. 5 (Suppl. 1), S12–S21.

del Zoppo, G.J., Hallenbeck, J.M., 2000. Advances in the vascular pathophysiology of ischemic stroke. Thromb. Res. 98, 73–81.

FitzGerald, G.A., 1987. Dipyridamole. N. Engl. J. Med. 316, 1247–1257.

Fujita, Y., Lin, J.X., Takahashi, R., Tomimoto, H., 2008. Cilostazol alleviates cerebral small-vessel pathology and white-matter lesions in stroke-prone spontaneously hypertensive rats. Brain Res. 1203, 170–176.

Fujita, Y., Ihara, M., Ushiki, T., Hirai, H., Kizaka-Kondoh, S., Hiraoka, M., Ito, H., Takahashi, R., 2010. Early protective effect of bone marrow mononuclear cells against ischemic white matter damage through augmentation of cerebral blood flow. Stroke 41, 2938–2943.

Gerber, J., Raivich, G., Wellmer, A., Noeske, C., Kunst, T., Werner, A., Bruck, W., Nau, R., 2001. A mouse model of Streptococcus pneumoniae meningitis mimicking several features of human disease. Acta Neuropathol. 101, 499–508.

Gotoh, F., Tohgi, H., Hirai, S., Terashi, A., Fukuuchi, Y., Otomo, E., Shinohara, Y., Itoh, E., Matsuda, T., Sawada, T., Yamaguchi, T., Nishimaru, K., Ohashi, Y., 2000. Cilostazol stroke prevention study: A placebo-controlled double-blind trial for secondary prevention of cerebral infarction. J. Stroke Cerebrovasc. Dis. 9, 147–157.

Halkes, P.H., van Gijn, J., Kappelle, L.J., Koudstaal, P.J., Algra, A., 2006. Aspirin plus dipyridamole versus aspirin alone after cerebral ischaemia of arterial origin (ESPRIT): randomised controlled trial. Lancet 367, 1665–1673.

Huang, Y., Cheng, Y., Wu, J., Li, Y., Xu, E., Hong, Z., Li, Z., Zhang, W., Ding, M., Gao, X., Fan, D., Zeng, J., Wong, K., Lu, C., Xiao, J., Yao, C., 2008. Cilostazol as an alternative to aspirin after ischaemic stroke: a randomised, double-blind, pilot study. Lancet Neurol. 7, 494–499.

Ishiguro, M., Mishiro, K., Fujiwara, Y., Chen, H., Izuta, H., Tsuruma, K., Shimazawa, M., Yoshimura, S., Satoh, M., Iwama, T., Hara, H., 2010. Phosphodiesterase-III inhibitor prevents hemorrhagic transformation induced by focal cerebral ischemia in mice treated with tPA. PLoS One 5, e15178.

Ito, H., Hashimoto, A., Matsumoto, Y., Yao, H., Miyakoda, G., 2010. Cilostazol, a phosphodiesterase inhibitor, attenuates photothrombotic focal ischemic brain injury in hypertensive rats. J. Cereb. Blood Flow Metab. 30, 343–351.

Kim, K.Y., Shin, H.K., Choi, J.M., Hong, K.W., 2002. Inhibition of lipopolysaccharide-induced apoptosis by cilostazol in human umbilical vein endothelial cells. J. Pharmacol. Exp. Ther. 300, 709–715.

Kollmar, R., Henninger, N., Bardutzky, J., Schellinger, P.D., Schabitz, W.R., Schwab, S., 2004. Combination therapy of moderate hypothermia and thrombolysis in experimental thromboembolic stroke–an MRI study. Exp. Neurol. 190, 204–212.

Komine-Kobayashi, M., Chou, N., Mochizuki, H., Nakao, A., Mizuno, Y., Urabe, T., 2004. Dual role of Fcgamma receptor in transient focal cerebral ischemia in mice. Stroke 35, 958–963.

Kothari, R.U., Brott, T., Broderick, J.P., Barsan, W.G., Sauerbeck, L.R., Zuccarello, M., Khoury, J., 1996. The ABCs of measuring intracerebral hemorrhage volumes. Stroke 27, 1304–1305.

Lee, J.H., Kim, K.Y., Lee, Y.K., Park, S.Y., Kim, C.D., Lee, W.S., Rhim, B.Y., Hong, K.W., 2004. Cilostazol prevents focal cerebral ischemic injury by enhancing casein kinase 2 phosphorylation and suppression of phosphatase and tensin homolog deleted from chromosome 10 phosphorylation in rats. J. Pharmacol. Exp. Ther. 308, 896–903.

Liu, Y., Shakur, Y., Yoshitake, M., Kambayashi Ji, J., 2001. Cilostazol (pletal): a dual inhibitor of cyclic nucleotide phosphodiesterase type 3 and adenosine uptake. Cardiovasc. Drug Rev. 19, 369–386.

Maddahi, A., Chen, Q., Edvinsson, L., 2009. Enhanced cerebrovascular expression of matrix metalloproteinase-9 and tissue inhibitor of metalloproteinase-1 via the MEK/ERK pathway during cerebral ischemia in the rat. BMC Neurosci. 10, 56.

Ohlstein, E.H., Storer, B., Fujita, T., Shebuski, R.J., 1987. Tissue-type plasminogen activator and streptokinase induce platelet hyperaggregability in the rabbit. Thromb. Res. 46, 575–585.

Shinohara, Y., Katayama, Y., Uchiyama, S., Yamaguchi, T., Handa, S., Matsuoka, K., Ohashi, Y., Tanahashi, N., Yamamoto, H., Genka, C., Kitagawa, Y., Kusuoka, H., Nishimaru, K., Tsushima, M., Koretsune, Y., Sawada, T., Hamada, C., 2010. Cilostazol for prevention of secondary stroke (CSPS 2): an aspirin-controlled, double-blind, randomised non-inferiority trial. Lancet Neurol. 9, 959–968.

Tanaka, K., Gotoh, F., Fukuuchi, Y., Amano, T., Uematsu, D., Kawamura, J., Yamawaki, T., Itoh, N., Obara, K., Muramatsu, K., 1989. Effects of a selective inhibitor of cyclic AMP phosphodiesterase on the pial microcirculation in feline cerebral ischemia. Stroke 20, 668–673.

Tanaka, Y., Tanaka, R., Liu, M., Hattori, N., Urabe, T., 2010. Cilostazol attenuates ischemic brain injury and enhances neurogenesis in the subventricular zone of adult mice after transient focal cerebral ischemia. Neuroscience 171, 1367–1376.

Tsai, C.S., Lin, F.Y., Chen, Y.H., Yang, T.L., Wang, H.J., Huang, G.S., Lin, C.Y., Tsai, Y.T., Lin, S.J., Li, C.Y., 2008. Cilostazol attenuates MCP-1 and MMP-9 expression in vivo in LPS-administrated balloon-injured rabbit aorta and in vitro in LPS-treated monocytic THP-1 cells. J. Cell. Biochem. 103, 54–66.

Uematsu, D., Greenberg, J.H., Reivich, M., Hickey, W.F., 1989. Direct evidence for calcium-induced ischemic and reperfusion injury. Ann. Neurol. 26, 280–283.

von Kummer, R., Bourquain, H., Bastianello, S., Bozzao, L., Manelfe, C., Meier, D., Hacke, W., 2001. Early prediction of irreversible brain damage after ischemic stroke at CT. Radiology 219, 95–100.

Wang, X., Lee, S.R., Arai, K., Tsuji, K., Rebeck, G.W., Lo, E.H., 2003. Lipoprotein receptor-mediated induction of matrix metalloproteinase by tissue plasminogen activator. Nat. Med. 9, 1313–1317.

Zhang, L., Schallert, T., Zhang, Z.G., Jiang, Q., Arniego, P., Li, Q., Lu, M., Chopp, M., 2002. A test for detecting long-term sensorimotor dysfunction in the mouse after focal cerebral ischemia. J. Neurosci. Methods 117, 207–214.